

STABILITY AND BIFURCATIONS IN NEURAL FIELDS WITH FINITE PROPAGATION SPEED AND GENERAL CONNECTIVITY*

FATİHCAN M. ATAY[†] AND AXEL HUTT[‡]

Abstract. A stability analysis is presented for neural field equations in the presence of finite propagation speed along axons and for a general class of connectivity kernels and synaptic properties. Sufficient conditions are given for the stability of equilibrium solutions. It is shown that the propagation delays play a significant role in nonstationary bifurcations of equilibria, whereas the stationary bifurcations depend only on the connectivity kernel. In the case of nonstationary bifurcations, bounds are determined on the frequencies of the resulting oscillatory solutions. A perturbative scheme is used to calculate the types of bifurcations leading to spatial patterns, oscillations, and traveling waves. For high propagation speeds a simple method is derived that allows the determination of the bifurcation type by visual inspection of the Fourier transforms of the kernel and its first moment. Results are numerically illustrated on a class of neurologically plausible systems with combinations of Gaussian excitatory and inhibitory connections.

Key words. synaptic networks, nonlocal interaction, delay, bifurcations, spatiotemporal patterns, traveling waves

AMS subject classifications. 92C20, 34K99, 37N25, 37G10

DOI. 10.1137/S0036139903430884

1. Introduction. In recent years, there has been growing interest in the mechanisms of spatiotemporal activity in neural tissue. In this field, applications of various experimental techniques [37, 21, 39, 41] revealed formations of different spatial patterns, traveling waves, and pulses [28, 43, 48], standing pulses (e.g., [18]), or irregular spatial patterns [2, 40]. Since neural tissue exhibits multiscale properties in space and time, the analysis of such activity represents a challenging task. However, reduced biological models at fixed scales in time and space simplify the analysis and allow for analytical treatments (see, e.g., [5, 12, 42] for review). In this context, a well-known approach is to focus on neuronal ensembles [46, 47, 29], which allows for the successful reconstruction of empirical data measured on a macroscopic scale [24, 30, 35, 34, 25].

On a small spatial level ($\sim 50\mu m$), model neurons may consist of two compartments: synapses, which convert incoming action potentials to postsynaptic potentials, and a trigger zone, where these potentials sum up and are reconverted to outgoing action potentials. Due to the large spatial density of neurons ($\sim 10^4$ neurons/mm³), one might consider ensemble activity on a larger spatial scale (> 1 mm), obtaining a coarse-grained description in space and time [46]. Consequently, macroscopic state variables of neuronal ensembles are mean pulse rates $P(x, t)$ and mean postsynaptic potentials $V(x, t)$, with x and t denoting the space and time coordinates, respectively. In the following, all quantities are meant to represent means of microscopic quantities.

Since the link between the microscopic description and the level of neural ensembles has been established in several previous works (e.g., [46, 38, 5, 4]), we only briefly

*Received by the editors June 30, 2003; accepted for publication (in revised form) April 6, 2004; published electronically January 5, 2005.

<http://www.siam.org/journals/siap/65-2/43088.html>

[†]Max Planck Institute for Mathematics in the Sciences, Inselstr. 22, Leipzig 04103, Germany (atay@member.ams.org).

[‡]Weierstrass Institute for Applied Analysis and Stochastics, Mohrenstr. 39, Berlin 10117, Germany (hutt@wias-berlin.de). The work of this author was supported by the DFG research center “Mathematics for key technologies” (FZT86), Berlin, Germany.

outline the basic mechanisms of activity conversion in neuronal fields. At chemical passive synapses, incoming pulse activity $J(x, t)$ is converted to postsynaptic potentials by convolution with an impulse response function $h(t)$, yielding

$$V(x, t) = \int_{-\infty}^t h(t - \tau)J(x, \tau)d\tau.$$

Since neuronal fields exhibit nonlocal interactions via axonal connections between synapses, incoming pulse activity obeys

$$J(x, t) = \beta \int_{\Omega} K(x, y)P(y, t - \Delta(x, y))dy + E(x, t),$$

where Ω is an appropriate spatial domain, K is the connectivity kernel, $\beta > 0$ is a scaling factor, and E is an additional external input. In the case of undamped axonal pulse propagation with finite velocity v and no additional constant delay, we get $\Delta(x, y) = |x - y|/v$. Essentially, the chain of activity conversion closes by the conversion of postsynaptic potentials to pulse rates

$$P(x, t) = S[V(x, t)],$$

where S is called the transfer function, which is taken to have a sigmoidal shape in most works. Considering all conversions, we obtain the integral equation

$$V(x, t) = \beta \int_{-\infty}^t \int_{\Omega} (h(t - \tau)K(x, y)S[V(y, \tau - |x - y|/v)] + E(x, \tau)) dy d\tau.$$

We then recast the impulse response function as a Green's function and thus stipulate

$$Lh(t) = \delta(t),$$

introducing a temporal differential operator L . Finally, we assume a homogeneous field where the connectivity $K(x, y)$ depends only on the distance $|x - y|$, and so we replace $K(x, y)$ by an even function $K(x - y)$. Hence, the final equation has the form

$$(1.1) \quad L(\partial/\partial t)V(x, t) = \beta \int_{\Omega} K(x - y)S(V(y, t - |x - y|/v)) dy + E(x, t),$$

where L is a polynomial and $L(\partial/\partial t)$ denotes a temporal differentiation operator with constant coefficients. We shall refer to (1.1) as an n th-order system, where $n \geq 1$ is the order of L .

The model (1.1) has been treated in the literature in several contexts and with different choices for L . In most studies the effect of transmission speed has been neglected by letting $v = \infty$ in the model, the justification being that the signal propagation is sufficiently fast or the spatial scales of the problem are small [32]. Some recent works [5, 15, 19, 31, 23, 8] have addressed the case of finite v by numerical investigations for particular choices of the kernel K . Our aim is to give an analytical treatment of the effects of finite transmission speeds for general K and L , in relation to the stability and bifurcation of the equilibrium solutions.

In the next section we consider the equilibrium solutions of (1.1) and give a sufficient condition for their stability. Section 3 discusses the types of dynamics that may emerge when stability is lost. Here it is shown that the transmission speed needs to

be smaller than a certain threshold in order to have oscillatory bifurcations in first- and second-order systems. Furthermore, bounds are calculated for the frequencies of the oscillatory solutions. In section 4, a perturbative analysis is used to compute the bifurcating solutions, and a graphical method is given to determine the possible bifurcations for a given kernel. Applications to kernels derived from Gaussian distributions are presented in section 5, and the paper concludes with a discussion of the results.

2. Stability of equilibrium solutions. For the rest of the paper we make the following assumptions regarding (1.1). For the spatial domain we assume $\Omega = \mathbf{R}$, although the results remain valid virtually without modification when Ω is a circle. The polynomial L is stable; i.e., all its roots have negative real parts. The kernel $K : \mathbf{R} \rightarrow \mathbf{R}$ is continuous, integrable, and even; that is, $K(-z) = K(z)$ for all $z \in \mathbf{R}$. Finally, the transfer function $S : \mathbf{R} \rightarrow \mathbf{R}$ is differentiable and monotone increasing.

It is often convenient to normalize the time and space in (1.1). For instance, if l and τ are some characteristic length and time of the physical problem, then one can define $\bar{t} = t/\tau$, $\bar{x} = x/l$, $\bar{V}(\bar{x}, \bar{t}) = V(l\bar{x}, \tau\bar{t})$, $\bar{E}(\bar{x}, \bar{t}) = E(l\bar{x}, \tau\bar{t})$, $\bar{L}(\partial/\partial\bar{t}) = \tau^n L(\tau^{-1}\partial/\partial t)$, $\bar{K}(\bar{z}) = K(lz)$, and $\bar{v} = \tau v/l$ so that (1.1) becomes

$$\bar{L}(\partial/\partial\bar{t})\bar{V}(\bar{x}, \bar{t}) = l\tau^n\beta \int_{\Omega} \bar{K}(\bar{x} - \bar{y})S(\bar{V}(\bar{y}, \bar{t}) - |\bar{x} - \bar{y}|/\bar{v}) d\bar{y} + \bar{E}(\bar{x}, \bar{t}),$$

which has the same form as (1.1). A common choice for characteristic time is $\tau^n = 1/L(0)$, in which case $\bar{L}(0) = 1$. Thus, without loss of generality we consider (1.1) with the assumption that $L(0) = 1$. Most studies of neuronal fields assume first- or second-order time derivatives in (1.1). To address these models in a unified manner, we shall often refer to the following specific form:

$$(2.1) \quad L(\lambda) = \eta\lambda^2 + \gamma\lambda + 1, \quad \eta = 0 \text{ or } 1, \quad \gamma > 0,$$

although certain results will be stated for arbitrary order stable polynomials L .

For a constant input $E(x, t) \equiv E^*$, an equilibrium solution $V(x, t) \equiv V^*$ satisfies

$$(2.2) \quad V^* = \beta \int_{-\infty}^{\infty} K(x - y)S(V^*) dy + E^*.$$

Let

$$(2.3) \quad \kappa = \int_{-\infty}^{\infty} K(z) dz = 2 \int_0^{\infty} K(z) dz.$$

Then (2.2) can be written as

$$(2.4) \quad f(V^*) \stackrel{\text{def}}{=} V^* - \kappa\beta S(V^*) = E^*.$$

If S is bounded, then $f : \mathbf{R} \rightarrow \mathbf{R}$ is surjective; thus (2.4) has a solution V^* for any $E^* \in \mathbf{R}$. The uniqueness of V^* depends on the sign of κ and the shape of S . If S is positive and increasing on \mathbf{R} , such as a sigmoid function, and if $\kappa \leq 0$, then f is increasing and hence also injective, in which case the solution V^* is unique. On the other hand, if $\kappa > 0$, then there may be multiple equilibria, as (2.4) can have more than one solution V^* for a given E^* .

The stability of the equilibrium solution V^* is determined by the linear variational equation

$$(2.5) \quad L(\partial/\partial t)u(x, t) = \alpha \int_{-\infty}^{\infty} K(x - y)u(y, t - |x - y|/v) dy,$$

where $u(x, t) = V(x, t) - V^*$ and $\alpha = \beta S'(V^*) \geq 0$. We shall use α as a bifurcation parameter in the following sections. Using the ansatz $u(x, t) = e^{\lambda t} \varphi(x)$ in (2.5) one obtains

$$(2.6) \quad L(\lambda)\varphi(x) = \alpha \int_{-\infty}^{\infty} K(x - y) \exp(-\lambda|x - y|/v)\varphi(y) dy.$$

Thus φ is an eigenfunction of an integral operator. Due to the difference kernel the eigenfunctions have the form $\varphi(x) = e^{ikx}$ for some $k \in \mathbf{R}$, and substituting into (2.6) followed by a change of variables $z = x - y$ in the integral gives

$$(2.7) \quad L(\lambda) = \alpha \int_{-\infty}^{\infty} K(z) \exp(-\lambda|z|/v) \exp(-ikz) dz.$$

The integral above is the Fourier transform of the function $K_\lambda(z) = K(z) \exp(-\lambda|z|/v)$ (up to a multiplicative factor, depending on which definition one uses), which is also equal to its cosine transform since $K_\lambda(z)$ is an even function of z . The dispersion relation (2.7) between the temporal and spatial modes λ and k is in general difficult to solve explicitly. A notable exception is the case of instantaneous information transmission, since when $v = \infty$, the right-hand side of (2.7) is independent of λ . In this paper we are interested in the effects of finite transmission speeds.

The solutions (λ, k) of (2.7) correspond to the perturbations $u(x, t) = e^{\lambda t} e^{ikx}$ about the equilibrium solution, which grow or decay in time depending on whether $\text{Re } \lambda$ is positive or negative, respectively, thus determining the stability of V^* . We give sufficient conditions for asymptotic stability.

THEOREM 2.1. *Let $c = \alpha \int_{-\infty}^{\infty} |K(z)| dz$. If*

$$(2.8) \quad c < \min_{\omega \in \mathbf{R}} |L(i\omega)|,$$

then V^ is asymptotically stable. In particular, if $L(\lambda) = \lambda + 1$, then the condition*

$$(2.9) \quad c < 1$$

is sufficient for the asymptotic stability of V^ . If $L(\gamma) = \lambda^2 + \gamma\lambda + 1$ with $\gamma > 0$, then V^* is asymptotically stable provided that the condition*

$$(2.10) \quad \frac{\gamma^2}{2} > 1 - \sqrt{1 - c^2}$$

holds, in addition to (2.9).

The following lemma will be useful in the proof of the theorem.

LEMMA 2.2. *Let $L(\lambda)$ be a polynomial whose roots have nonpositive real parts. Then*

$$|L(\sigma + i\omega)| \geq |L(i\omega)|$$

for all $\sigma \geq 0$ and $\omega \in \mathbf{R}$.

Proof. If λ_k denote the roots of L , then $L(\lambda) = (\lambda - \lambda_1)(\lambda - \lambda_2) \cdots (\lambda - \lambda_n)$, where n is the order of L . Thus

$$\begin{aligned} |L(\sigma + i\omega)| &= \prod_{k=1}^n |\sigma + i\omega - \lambda_k| \\ &= \prod_{k=1}^n ((\sigma - \operatorname{Re}[\lambda_k])^2 + (\omega - \operatorname{Im}[\lambda_k])^2)^{1/2}. \end{aligned}$$

By assumption, $\sigma \geq 0$ and $\operatorname{Re}[\lambda_k] \leq 0$ for all k , so

$$\begin{aligned} |L(\sigma + i\omega)| &\geq \prod_{k=1}^n ((-\operatorname{Re}[\lambda_k])^2 + (\omega - \operatorname{Im}[\lambda_k])^2)^{1/2} \\ &= \prod_{k=1}^n |i\omega - \lambda_k| \\ &= |L(i\omega)|. \quad \square \end{aligned}$$

Proof of Theorem 2.1. In the ansatz $u(x, t) = e^{\lambda t} e^{ikx}$, let $\lambda = \sigma + i\omega$, where σ and ω are real numbers. We will prove that $\sigma < 0$ if (2.8) holds. Suppose by way of contradiction that (2.8) holds but $\sigma \geq 0$. From the dispersion relation (2.7) it follows that

$$\begin{aligned} |L(\sigma + i\omega)| &= \alpha \left| \int_{-\infty}^{\infty} K(z) \exp(-(\sigma + i\omega)|z|/v) \exp(-ikz) dz \right| \\ &\leq \alpha \int_{-\infty}^{\infty} |K(z)| |\exp(-(\sigma + i\omega)|z|/v)| dz \\ (2.11) \quad &\leq \alpha \int_{-\infty}^{\infty} |K(z)| dz = c. \end{aligned}$$

On the other hand, by Lemma 2.2,

$$|L(i\omega)| \leq |L(\sigma + i\omega)|,$$

which together with (2.11) implies

$$|L(i\omega)| \leq c$$

for some $\omega \in \mathbf{R}$. This, however, contradicts (2.8). Thus $\sigma < 0$, and the equilibrium solution is asymptotically stable. This proves the first statement of the theorem. In the specific case when L is given by $L(\lambda) = \lambda + 1$, one has $|L(i\omega)|^2 = 1 + \omega^2$. Hence if (2.9) is satisfied, then

$$c^2 < 1 \leq 1 + \omega^2 = |L(i\omega)|^2 \quad \text{for all } \omega \in \mathbf{R},$$

which is a sufficient condition for stability by (2.8). Similarly, suppose that L has the form $L(\lambda) = \lambda^2 + \gamma\lambda + 1$ and that (2.9) and (2.10) are satisfied. Then

$$|L(i\omega)|^2 = (1 - \omega^2)^2 + (\gamma\omega)^2.$$

Now consider the function

$$\begin{aligned} g(\omega) &\stackrel{\text{def}}{=} |L(i\omega)|^2 - c^2 \\ (2.12) \quad &= \omega^4 + (\gamma^2 - 2)\omega^2 + (1 - c^2). \end{aligned}$$

If $\gamma^2 \geq 2$, then $g(\omega)$ is positive for all ω by (2.9). On the other hand, if $\gamma^2 < 2$, then by (2.10)

$$0 < 2 - \gamma^2 < 2\sqrt{1 - c^2},$$

implying that the discriminant $(\gamma^2 - 2)^2 - 4(1 - c^2)$ is negative; thus g has no real roots. Thus, in either case, $g(\omega)$ is positive, or, equivalently, $c < |L(i\omega)|$ for all ω , and stability again follows by the first statement of the theorem. \square

3. Bifurcations. When $\alpha = 0$, the eigenvalues λ are simply given by the roots of L , so that $\text{Re } \lambda < 0$ by the assumption that L is a stable polynomial, and the equilibrium point is asymptotically stable. As α is increased, stability can be lost if an eigenvalue λ crosses the imaginary axis. At the critical transition there is an eigenvalue of the form $\lambda = i\omega$, $\omega \in \mathbf{R}$, and the dispersion relation (2.7) has the form

$$(3.1) \quad L(i\omega) = \alpha \int_{-\infty}^{\infty} K(z) \exp(-i(kz + \omega|z|/v)) dz.$$

The possibilities for the resulting behavior when α is near such a critical value can then be qualitatively classified as follows:

I. Stationary bifurcations

- a. $\omega = 0$ and $k = 0$: bifurcation to a spatially and temporally constant solution.
- b. $\omega = 0$ and $k \neq 0$: bifurcation to a spatially periodic solution which is constant in time, leading to spatial patterns (Turing modes).

II. Nonstationary bifurcations

- a. $\omega \neq 0$ and $k = 0$: Hopf bifurcation to periodic oscillations of a spatially uniform solution.
- b. $\omega \neq 0$ and $k \neq 0$: bifurcation to traveling waves, with wave speed equal to ω/k .

The conditions for stationary bifurcations are easily characterized by the relation (3.1), recalling the assumption that $L(0) = 1$. Thus for case Ia one has

$$(3.2) \quad 1 = \alpha \int_{-\infty}^{\infty} K(z) dz = \alpha\kappa$$

with κ as defined in (2.3). This is only possible if $\kappa > 0$ and is the mechanism for appearance of multiple equilibrium solutions of (2.2). Similarly, the condition (2.7) for case Ib is

$$(3.3) \quad 1 = \alpha \int_{-\infty}^{\infty} K(z) \exp(ikz) dz = \alpha\hat{K}(k), \quad k \neq 0,$$

where \hat{K} denotes the Fourier transform of K . As α is increased from zero, the first mode that becomes unstable in the linearized equation is expected to give an indication of what would be observed in the full nonlinear system (1.1). Hence, spatial patterns are typically observed as bifurcations from equilibria if a nonzero k is the first mode that loses stability. From (3.3) it follows that a necessary condition for this is that the maximum value of the Fourier transform of K is positive and occurs at a nonzero frequency k .

It is clear from (3.2) and (3.3) that stationary bifurcations are independent of the order of the temporal differentiation operator L or the transmission speed v . Their

analysis only involves the properties of the Fourier transform of the kernel function. On the other hand, L and v turn out to be crucial in nonstationary bifurcations. Indeed, our next result shows that a sufficiently small transmission speed is actually a necessary condition for nonstationary bifurcations in first- and second-order systems.

THEOREM 3.1. *Suppose $L(\lambda) = \eta\lambda^2 + \gamma\lambda + 1$, where η may possibly be zero. If*

$$(3.4) \quad v > \frac{\alpha}{|\gamma|} \int_{-\infty}^{\infty} |zK(z)| dz,$$

then (2.5) has no solutions of the form $u(x, t) = \exp i(\omega t + kx)$ with ω real and nonzero.

Proof. From the dispersion relation (2.7),

$$\begin{aligned} L(\lambda) &= \alpha \int_{-\infty}^{\infty} K(z) \exp(-\lambda|z|/v) (\cos kz - i \sin kz) dz \\ &= \alpha \int_{-\infty}^{\infty} K(z) \exp(-\lambda|z|/v) \cos kz dz \end{aligned}$$

since the function $K(z) \exp(-\lambda|z|/v)$ is even in z . Separating the real and imaginary parts of the above expression at the bifurcation value $\lambda = i\omega$ gives

$$(3.5) \quad \operatorname{Re} L(i\omega) = \alpha \int_{-\infty}^{\infty} K(z) \cos(\omega z/v) \cos(kz) dz,$$

$$(3.6) \quad \operatorname{Im} L(i\omega) = -\alpha \int_{-\infty}^{\infty} K(z) \sin(\omega|z|/v) \cos(kz) dz.$$

Suppose $L(\lambda) = \eta\lambda^2 + \gamma\lambda + 1$. Then $\operatorname{Im} L(i\omega) = \gamma\omega$, and (3.6) implies

$$\begin{aligned} |\gamma\omega| &= \alpha \left| \int_{-\infty}^{\infty} K(z) \sin(\omega|z|/v) \cos(kz) dz \right| \\ &\leq \alpha \int_{-\infty}^{\infty} |K(z) \sin(\omega z/v)| dz \\ &\leq \alpha \int_{-\infty}^{\infty} |K(z)\omega z/v| dz, \end{aligned}$$

where we have used the estimate $|\sin(x)| \leq |x|$ for all $x \in \mathbf{R}$. If $\omega \neq 0$, then $|\omega|$ may be cancelled in the last inequality to yield

$$|\gamma| \leq \frac{\alpha}{v} \int_{-\infty}^{\infty} |zK(z)| dz.$$

This, however, contradicts the assumption (3.4). Hence $\omega = 0$, which proves the theorem. \square

We note that the above result is valid for first- and second-order systems; in higher order systems, bifurcation values $\lambda = i\omega \neq 0$ may occur even with $v = \infty$ [12].

For bifurcating oscillatory solutions, it is possible to put a priori bounds on the possible values of the frequencies ω in terms of the kernel function and the operator L , as given by the next result.

THEOREM 3.2. *Let c be as defined in Theorem 2.1. Then there exists $B > 0$, depending only on L and c , such that*

$$(3.7) \quad |\omega| \leq B$$

whenever $u(x, t) = \exp i(\omega t + kx)$, $\omega, k \in \mathbf{R}$, is a solution of (2.5). Furthermore, if $c < 1$, then there exists $A > 0$, depending only on L and c , such that

$$(3.8) \quad 0 < A \leq |\omega|.$$

In particular, if $L(\lambda) = \lambda + 1$, then

$$(3.9) \quad \omega^2 \leq c^2 - 1,$$

and if $L(\lambda) = \lambda^2 + \gamma\lambda + 1$, then

$$(3.10) \quad \begin{aligned} (1 - \frac{1}{2}\gamma^2) - \delta \leq \omega^2 \leq (1 - \frac{1}{2}\gamma^2) + \delta & \text{ if } 0 \leq c < 1, \\ 0 \leq \omega^2 \leq (1 - \frac{1}{2}\gamma^2) + \delta & \text{ if } c \geq 1, \end{aligned}$$

where $\delta = \sqrt{(1 - \frac{1}{2}\gamma^2)^2 - 1 + c^2}$.

Remark. The existence of a solution of the form $u(x, t) = \exp i(\omega t + kx)$ implies that the equilibrium point is not asymptotically stable. It is then a consequence of Theorem 2.1 that the right sides of the inequalities in (3.9) and (3.10) are nonnegative.

Proof of Theorem 3.2. If $\lambda = i\omega$ satisfies the dispersion relation (2.7) for some k , then

$$(3.11) \quad |L(i\omega)| \leq \alpha \int_{-\infty}^{\infty} |K(z)| dz = c.$$

Since $|L(i\omega)| \rightarrow \infty$ as $\omega \rightarrow \pm\infty$ for any nonconstant polynomial L , the above inequality implies an upper bound B on $|\omega|$, which proves (3.7). For the particular case when $L(\lambda) = \lambda + 1$, (3.11) gives

$$|L(i\omega)|^2 = \omega^2 + 1 \leq c^2,$$

proving (3.9). Similarly, for $L(\lambda) = \lambda^2 + \gamma\lambda + 1$, (3.11) yields

$$(3.12) \quad |L(i\omega)|^2 = \omega^4 + (\gamma^2 - 2)\omega^2 + 1 \leq c^2.$$

If we let $u = \omega^2$, then the inequality above is equivalent to saying that possible values of $u \geq 0$ are those which render the function

$$h(u) \stackrel{\text{def}}{=} u^2 + (\gamma^2 - 2)u + (1 - c^2)$$

negative or zero. This is only possible if h has at least one root in the interval $[0, \infty)$, implying that the discriminant $(\gamma^2 - 2)^2 - 4(1 - c^2)$ is nonnegative. Letting $\delta = \sqrt{(1 - \frac{1}{2}\gamma^2)^2 - 1 + c^2}$, the roots of h can be written as $(1 - \frac{1}{2}\gamma^2) \pm \delta$. Thus $h(\omega^2) \leq 0$ for ω^2 satisfying

$$(3.13) \quad (1 - \frac{1}{2}\gamma^2) - \delta \leq \omega^2 \leq (1 - \frac{1}{2}\gamma^2) + \delta.$$

It remains to ensure that the interval above is a subset of $[0, \infty)$. If $c < 1$, then it is easy to see that both roots of h are nonnegative. For if the smaller root is negative, we have

$$0 > (1 - \frac{1}{2}\gamma^2) - \delta > (1 - \frac{1}{2}\gamma^2) - |1 - \frac{1}{2}\gamma^2|,$$

so $(1 - \frac{1}{2}\gamma^2) < 0$. But then both the conditions (2.9) and (2.10) are satisfied, and by Theorem 2.1 $\lambda = i\omega$ cannot be a solution to (2.7). On the other hand, if $c \geq 1$, then

$$(1 - \frac{1}{2}\gamma^2) - \delta \leq (1 - \frac{1}{2}\gamma^2) - |1 - \frac{1}{2}\gamma^2| \leq 0$$

and

$$(1 - \frac{1}{2}\gamma^2) + \delta \geq (1 - \frac{1}{2}\gamma^2) + |1 - \frac{1}{2}\gamma^2| \geq 0.$$

So, in this case the lower bound on ω^2 in (3.13) can be replaced by zero. This establishes (3.10). Finally, to prove (3.8) for arbitrary L assume that $c < 1$. Then $1 = L(0) > c$. By the continuity of L there exists $A > 0$ such that $|L(i\omega)| > c$ whenever $|\omega| \leq A$. Since (3.11) is not satisfied, (2.5) does not have a solution of the form $\exp i(\omega t + kx)$ with $|\omega| \leq A$, which completes the proof. \square

4. Perturbative analysis. In order to study the type of bifurcations that may arise in a given situation, the dispersion relation (3.1) needs to be solved for ω and k . However, explicit solutions are difficult to obtain for general kernel functions. The results of the previous sections imply that in the absence of delays, one has a simpler case, where nonstationary bifurcations do not exist in first- and second-order systems. Consequently, the role of delays can be systematically examined by following the changes in the bifurcation structure as the value of the transmission speed is decreased from infinity. Hence we introduce the parameter $\varepsilon = 1/v$ and consider the change in dynamics as ε is increased from zero. This leads to an approximation scheme that provides valuable insight into the effects of axonal delays in the dynamics of the system.

Consider the power series estimate

$$\exp(-\lambda|z|/v) = \sum_{m=0}^N \frac{(-\lambda|z|/v)^m}{m!} + \mathcal{O}(v^{-(N+1)}).$$

Substitution in the dispersion relation (2.7) at the bifurcation value $\lambda = i\omega$ gives a finite series in powers of $\varepsilon = 1/v$,

$$\begin{aligned} L(i\omega) &= \alpha \int_{-\infty}^{\infty} K(z) \exp(-ikz) \left[\sum_{m=0}^N \frac{(-i\varepsilon\omega|z|)^m}{m!} + \mathcal{O}(\varepsilon^{N+1}) \right] dz \\ (4.1) \quad &= \alpha \sum_{m=0}^N \frac{(-i\varepsilon\omega)^m}{m!} \hat{K}_m(k) + \mathcal{O}(\varepsilon^{N+1}), \end{aligned}$$

where the \hat{K}_m denote the transforms of the moments of K :

$$(4.2) \quad \hat{K}_m(k) = \int_{-\infty}^{\infty} |z|^m K(z) \exp(-ikz) dz = 2 \int_0^{\infty} z^m K(z) \cos(kz) dz$$

and the integrals are assumed to exist. Separating the real and imaginary parts of (4.1) then yields

$$(4.3) \quad \alpha^{-1} \operatorname{Re} L(i\omega) = \hat{K}_0(k) - \frac{\varepsilon^2}{2} \omega^2 \hat{K}_2(k) + \frac{\varepsilon^4}{24} \omega^4 \hat{K}_4(k) - \dots,$$

$$(4.4) \quad \alpha^{-1} \operatorname{Im} L(i\omega) = -\varepsilon\omega \hat{K}_1(k) + \frac{\varepsilon^3}{6} \omega^3 \hat{K}_3(k) - \frac{\varepsilon^5}{120} \omega^5 \hat{K}_5(k) + \dots.$$

The number of terms needed for the above series to be useful depends on the value of ε as well as the shape of the kernel K . If K is highly concentrated near the origin, then a few terms are sufficient. To make this precise, suppose that K is of exponential order, which is a reasonable assumption in most practical situations. In other words, suppose there exist positive numbers κ_1 and κ_2 such that

$$|K(z)| \leq \kappa_1 \exp(-\kappa_2|z|) \quad \text{for all } z \in \mathbf{R}.$$

Then, by (4.2),

$$\begin{aligned} \left| \hat{K}_m(k) \right| &\leq \int_{-\infty}^{\infty} |z|^m \kappa_1 \exp(-\kappa_2|z|) dz = 2\kappa_1 \int_0^{\infty} z^m \exp(-\kappa_2 z) dz \\ &= 2\kappa_1 \kappa_2^{-(m+1)} \Gamma(m+1) = 2\kappa_1 \kappa_2^{-(m+1)} m!, \end{aligned}$$

so the m th term in the series (4.1) is bounded in absolute value by

$$2 \frac{\kappa_1}{\kappa_2} \left(\frac{\varepsilon|\omega|}{\kappa_2} \right)^m \leq 2 \frac{\kappa_1}{\kappa_2} \left(\frac{B}{\kappa_2} \varepsilon \right)^m,$$

where we have used Theorem 3.2 to bound the values of ω . Hence, in case of small ε (large transmission speed) or B (e.g., small α) or a large value of κ_2 (fast decay of K away from the origin), the finite series has increased accuracy. We assume that at least one of these conditions is satisfied so that a small number of terms suffices to determine the general behavior.

In order to observe the qualitative effects of finite transmission speed, we thus neglect third- and higher order terms in ε in the series (4.1). Then, for L given by

$$L(\lambda) = \eta\lambda^2 + \gamma\lambda + 1, \quad \eta = 0 \text{ or } 1, \quad \gamma > 0,$$

(4.3)–(4.4) become

$$(4.5) \quad \alpha^{-1}(1 - \eta\omega^2) = \hat{K}(k) - \frac{1}{2}\varepsilon^2\omega^2 \hat{K}_2(k),$$

$$(4.6) \quad \alpha^{-1}\gamma\omega = -\varepsilon\omega \hat{K}_1(k),$$

where we have substituted the more conventional notation \hat{K} for the Fourier transform \hat{K}_0 of the kernel. For stationary bifurcations ($\omega = 0$), one obtains from the first equation that

$$(4.7) \quad \hat{K}(k) = 1/\alpha,$$

which is the same as the conditions (3.2)–(3.3) given by exact calculation. For a nonstationary bifurcation, $\omega \neq 0$, so (4.6) implies that

$$(4.8) \quad \hat{K}_1(k^*) = -\gamma/\varepsilon\alpha.$$

If $\hat{K}_1(k)$ assumes negative values, then it has a minimum since it is continuous and tends to zero as $k \rightarrow \pm\infty$; this minimum value corresponds to the first mode that loses stability as ε or α is increased. More precisely, if

$$(4.9) \quad k^* = \min_k \hat{K}_1(k) = \min_k \int_{-\infty}^{\infty} |z|K(z) \exp(-ikz) dz$$

exists and $\hat{K}_1(k^*) < 0$, then k^* is the sought solution of (4.8). Substituting k^* into (4.5) gives

$$(4.10) \quad \omega^2 = \frac{\alpha \hat{K}(k^*) - 1}{\frac{1}{2} \alpha \varepsilon^2 \hat{K}_2(k^*) - \eta},$$

which has a solution for ω whenever the right-hand side is nonnegative. This gives a simple procedure to calculate the pairs (ω, k) satisfying the dispersion relation and corresponding to the bifurcating solution $\exp(\omega t + kx)$.

It remains to determine what type of bifurcation actually occurs. This depends on the mode by which the equilibrium solution, which is stable for $\alpha = 0$, loses its stability as the bifurcation parameter α is increased. The procedure described in the above paragraph gives a simple graphical method. Thus if one plots the curves $\hat{K}(k)$ and $-\hat{K}_1(k)/\gamma v$ in the same graph and thinks of $1/\alpha$ as a horizontal line being lowered from $+\infty$, then the first intersection point specifies the bifurcation type. If the horizontal line touches the graph of $\hat{K}(k)$ first, then (4.7) is satisfied and a stationary bifurcation occurs. If, on the other hand, it touches $-\hat{K}_1(k)/\gamma v$ first, then (4.8) is satisfied and a nonstationary bifurcation occurs. Furthermore, the value of k at the intersection point being zero or nonzero specifies whether the bifurcating solution is spatially constant or not, respectively. It is worthwhile to note that the types of bifurcations that can occur depends only the extremal values of \hat{K} and \hat{K}_1 and not on the exact shapes of their graphs. This observation has two important consequences. First, the bifurcation structure depends on some general qualities of the kernel and not on its precise shape. And second, although our analysis is based on an approximation scheme, the qualitative conclusions regarding the type of bifurcations are generally robust, except for some degenerate cases, such as when the maximum values of $\hat{K}(k)$ and $-\hat{K}_1(k)/\gamma v$ are equal.

An example for the investigation of possible bifurcations is illustrated in Figure 1 for some typical kernel functions representing the possibilities for different types of inhibitory and excitatory interaction within the field. For each kernel type in the first column of the figure, the corresponding graphs of $\hat{K}(k)$ and $-\hat{K}_1(k)/\gamma v$ are plotted in the second column. By the argument outlined above, the possible bifurcations for each type of kernel can be directly read off from the graphs in the second column. The actual graphs in the figure are calculated from Gaussian distributions; however, it is clear that small variations in the graphs do not change the bifurcation types. In this way, it is possible to draw some general conclusions concerning different interaction kernels.

The analysis presented in this section is useful for understanding the relationship between the interactions within the field and the resulting dynamics. The stationary bifurcations of equilibria are determined by the Fourier transform \hat{K} of the connectivity kernel. The nonstationary bifurcations, on the other hand, are characterized by the transforms of the moments of the kernel. For first- and second-order systems this characterization can be reduced to the consideration of the single term $\hat{K}_1/\gamma v$, over the parameter ranges where the approximation scheme is justified. Outside of this range, e.g., for very low transmission speeds, more terms need to be considered in the series (4.1), together with a numerical solution of the system (4.3)–(4.4). Nevertheless, already in the term $\hat{K}_1/\gamma v$ one can see the ingredients responsible for nonstationary bifurcations: the operator L (through γ) representing the local temporal behavior, the kernel (through \hat{K}_1) representing spatial interaction, and the transmission speed v connecting the two aspects of the dynamics. Figure 1 gives a summary of the bifurcations resulting from the interplay of these elements. In the next section we

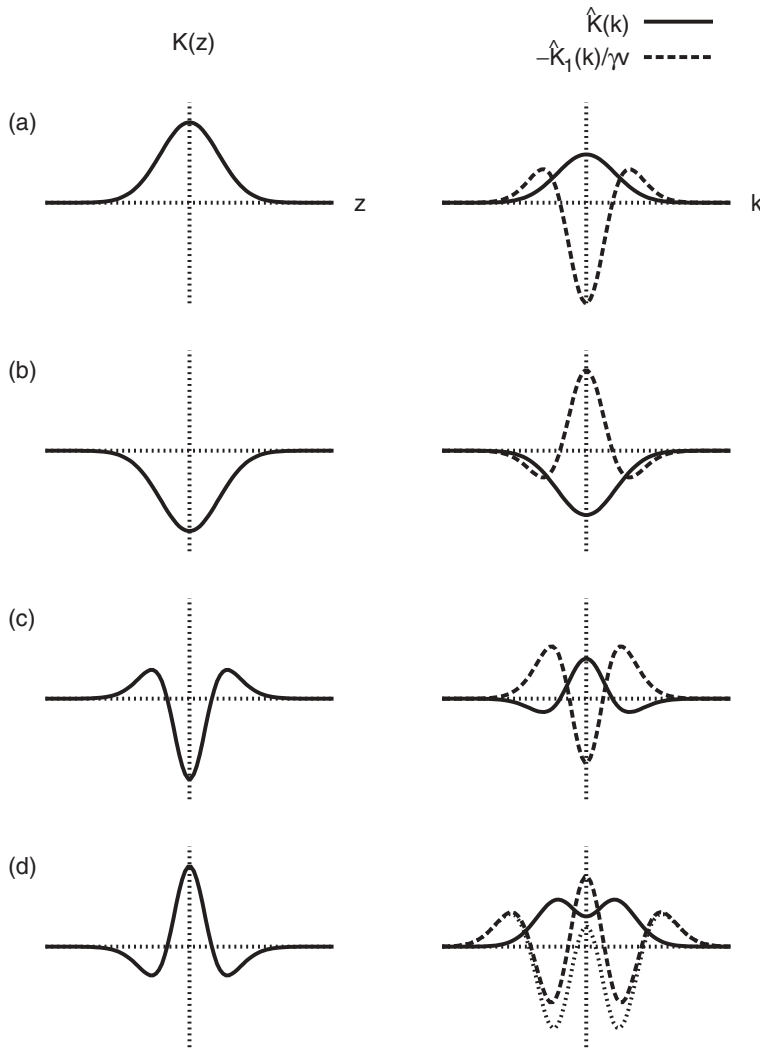


FIG. 1. Typical interaction kernels and possible bifurcation types. The first column shows the kernels, with the corresponding Fourier transforms in the second column. The maxima of \hat{K} and $-\hat{K}_1/\gamma\nu$, respectively, determine the stationary and oscillatory bifurcations, the largest peak giving the actual bifurcation taking place as α is increased. Hence, depending on the value of $\gamma\nu$, some typical cases are (a) an excitatory field, possible bifurcations Ia and IIb; (b) an inhibitory field, possible bifurcation IIa; (c) local inhibition and lateral excitation, possible bifurcations Ia and IIb; (d) local excitation and lateral inhibition, possible bifurcations Ib and IIa or IIb. In the last subfigure, two distinct possibilities for $-\hat{K}_1/\gamma\nu$ are shown with dashed and dotted lines.

present numerical simulations for the corresponding dynamical behavior in the non-linear system (1.1), obtained on the basis of the foregoing analysis.

5. Applications. We now examine the previous results numerically for a particular model. To this end, we set the differential operator to

$$(5.1) \quad L\left(\frac{\partial}{\partial t}\right) = \frac{\partial^2}{\partial t^2} + \gamma \frac{\partial}{\partial t} + 1$$

and further specify the connectivity kernel. Since a neuronal field might exhibit excitatory and inhibitory connections, the kernel K contains both excitatory and inhibitory distributions over space. In case of a homogeneous and isotropic neuronal field, a choice of K is

$$(5.2) \quad K(z) = \frac{1}{\sqrt{\pi}}(a_e e^{-z^2} - a_i r e^{-r^2 z^2}),$$

where a_e, a_i denote excitatory and inhibitory synaptic weights and $r = \sigma_e/\sigma_i$ gives the relation of excitatory and inhibitory spatial connectivity ranges σ_e and σ_i . Since the present work treats dynamics on a mesoscopic spatial scale, it does not resolve single synapses and synaptic interaction is considered in terms of normalized distributions of excitatory and inhibitory connections as in (5.2). Thus a purely excitatory connection (Figure 1(a)) is obtained when $a_i = 0$ and $a_e > 0$, whereas the choice $a_e = 0$ and $a_i > 0$ gives an inhibitory connection (Figure 1(b)). Similarly, for $a_e > a_i > 0$, local inhibition and lateral excitation (Figure 1(c)) or local excitation and lateral inhibition (Figure 1(d)) can be obtained by choosing $r > a_e/a_i$ or $0 < r < 1$, respectively. We shall mostly focus on these last two cases. Finally, we take $\beta = 1$ and choose the transfer function in (1.1) as the sigmoid $S(y) = 1/(1 + \exp(-1.8(y - 3)))$ according to previous works [46, 36].

The subsequent temporal integration procedure applies a fourth-order Runge–Kutta algorithm, while the spatial integration algorithm discretizes the field into N intervals and applies

$$(5.3) \quad \int_0^l f(z) dz \approx \sum_{i=1}^N \frac{1}{2}(f(z_i) + f(z_{i+1}))\Delta x$$

for any function f , with l the field length and $\Delta x = l/N$. Further, for periodic boundary conditions, the integration obeys the circular rule

$$(5.4) \quad \int_{-\infty}^{\infty} K(|x - y|)f(y)dy \approx \int_0^l K(l/2 - |l/2 - |x - y||)f(y)dy.$$

5.1. Stability of V^* . The equilibria V^* are found from (2.4). Figure 2 shows solutions V^* of (2.4) with respect to the external input for various values of κ . In the case where $\kappa > 2.2$, there exist up to three solutions A, B, and C subject to the external input, whereas there is only a single solution for $\kappa \leq 2.2$. Theorem 2.1 gives a sufficient condition for the stability of these equilibria. Note that for $\gamma > \sqrt{2}$ the inequality (2.10) is automatically satisfied, so $c < 1$ is a sufficient condition for asymptotic stability by the theorem. From (5.2) we have

$$(5.5) \quad c = \alpha|2a_e\Phi(x_0) - 2a_i\Phi(x_0r) - (a_e - a_i)|, \quad x_0 = \sqrt{\frac{1}{1-r^2} \ln\left(\frac{a_e}{a_i r}\right)},$$

where Φ is the Gaussian error function and $0 < r < 1$ or $r > a_e/a_i$. The spatial distance x_0 marks the change of sign of the kernel function and thus separates inhibitory from excitatory connections. The external input E^* affects c through $\alpha = S'(V^*)$. In Figure 3, c is plotted with respect to the input E^* for $r = 0.5$ and various parameter values of a_e, a_i at the different equilibria V^* . Stability is guaranteed by Theorem 2.1 at least in the region $c < 1$. In this line, Figure 4 shows a space-time plot of field

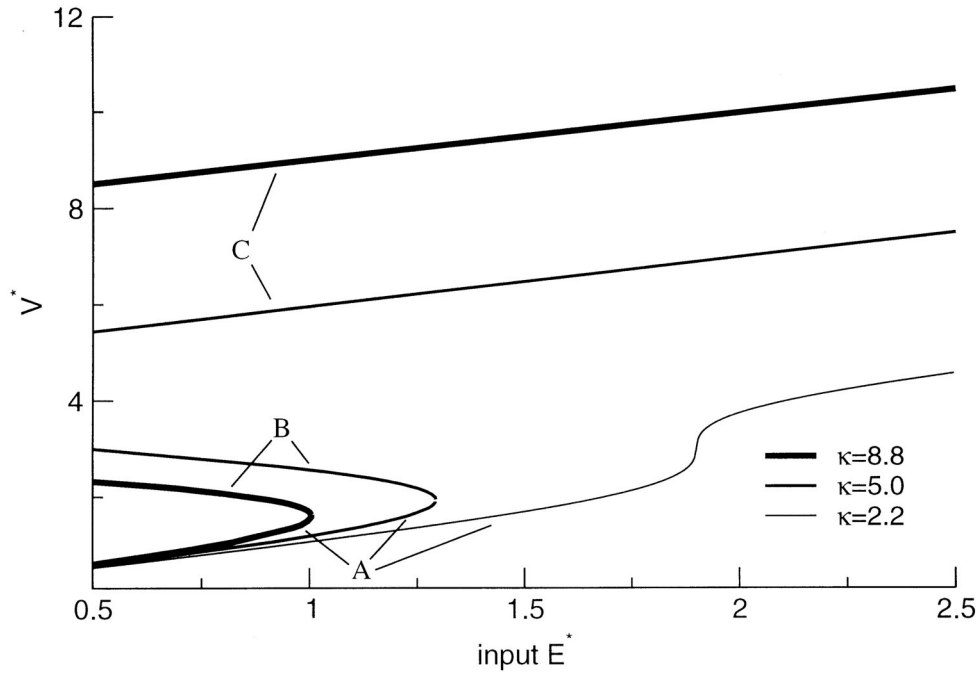


FIG. 2. Stationary constant fields V^* plotted with respect to the external input E^* for various parameters κ . Up to three solutions A, B, and C may exist for a given input level.

activity that relaxes to a lower solution A for $c = 0.85$ (cf. Figure 2). On the other hand, at sufficiently high values of α (and thus of c), stability is lost since when

$$(5.6) \quad \alpha = \frac{1}{\kappa},$$

the condition (3.2) for a type Ia bifurcation, is satisfied. This bifurcation point is also indicated in Figure 3. Therefore, the constant solutions denoted B in Figures 2–3 are unstable. Interestingly, this general result shows accordance to findings in previous works for special connectivity kernels [36, 23]. Finally, in the region $c > 1$ and $\alpha < 1/\kappa$, additional bifurcations might occur, yielding loss of stability. These are discussed in the following section.

5.2. Bifurcations. Recall that the external input defines the set of constant fields V^* , which subsequently determine the value of α ; hence α is an appropriate bifurcation parameter. For bifurcations to periodic patterns (Turing case Ib), the threshold condition from (3.3) reads

$$(5.7) \quad \alpha_{\text{thr}} = \frac{1}{a_e e^{-k_0^2/4} - a_i e^{-k_0^2/4r^2}}, \quad k_0^2 = \frac{4r^2}{r^2 - 1} \ln \frac{a_e r^2}{a_i},$$

where $k_0 = \arg \max_k \hat{K}(k)$. As $\alpha > 0$, we obtain directly from (5.7) that $r < 1$, i.e., there is no Turing instability for $r > 1$. Figure 5 displays thresholds α_{thr} with respect to parameters r , confirming this finding. Figure 6 displays a space-time plot of the corresponding Turing instability with $r = 0.5$.

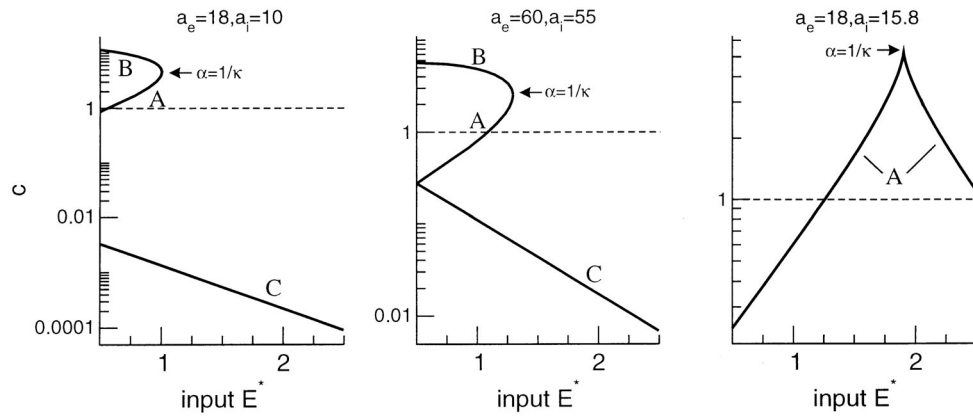


FIG. 3. Parameter c from Theorem 2.1 plotted with respect to the external input E^* for various parameters a_e, a_i and $r = 0.5, \gamma > \sqrt{2}$. The characters A, B, and C denote stationary solutions (see Figure 2) and solutions in the region below the dashed line fulfill the sufficient condition of asymptotic stability. It turns out that stationary solutions C are asymptotically stable for all external inputs in case of $a_e = 18, a_i = 10$ and $a_e = 60, a_i = 55$.

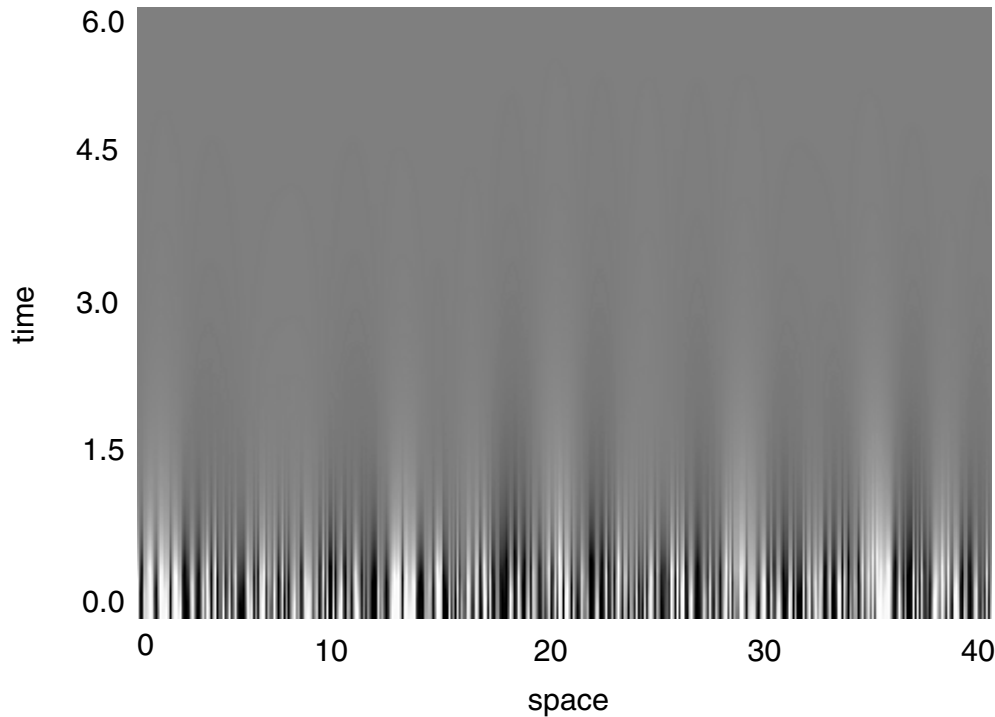


FIG. 4. Space-time plot of an asymptotically stable field for the Gaussian connectivity kernel and parameters $E^* = 0.5, r = 0.5, \gamma = 2, a_e = 60, a_i = 55, v = 100, \beta = 1, N = 400$. Initial values $V^0(x, t)$ are chosen randomly from a uniform distribution on $[V^* - 0.1, V^* + 0.1]$ for $t \in [-l/v, 0]$, where $l = 40$. The gray scale encodes the deviations from the stationary solution.

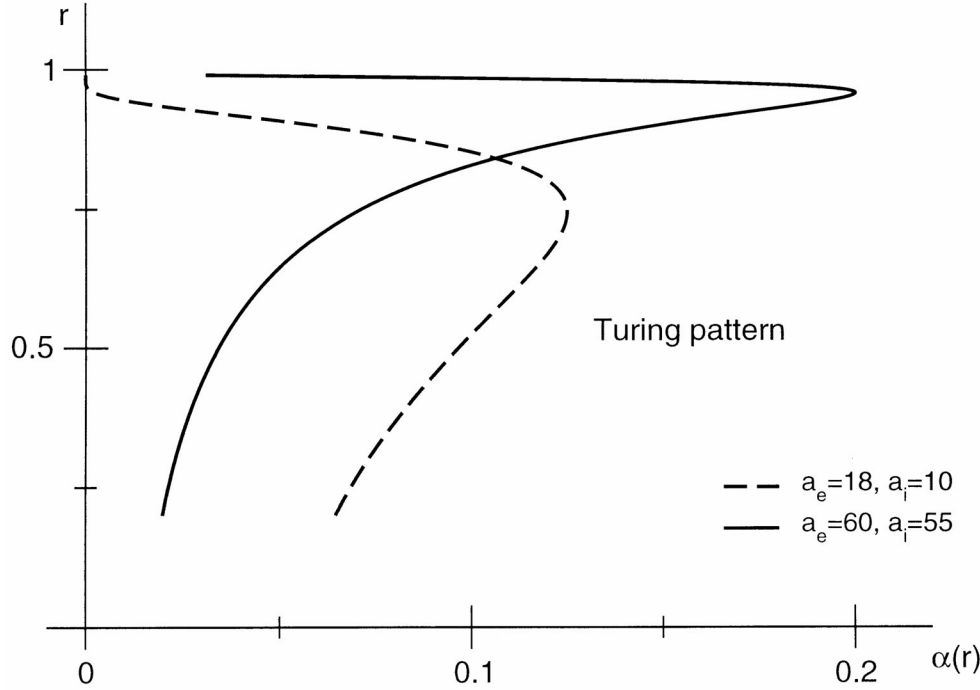


FIG. 5. Thresholds of stationary Turing bifurcations α_{thr} plotted for two parameter sets a_e, a_i . The regime of the Turing instability obeys $\alpha > \alpha_{\text{thr}}$, i.e., the right-hand side of each curve. The thresholds α_{thr} are independent from the synaptic parameter γ and the propagation speed v , while the external input E^* determines α implicitly.

Next, we consider oscillatory phenomena. From Theorem 3.1, a necessary condition for oscillatory behavior is

$$(5.8) \quad v < v_{\text{thr}} = \frac{\alpha}{|\gamma|\sqrt{\pi}} \left[\frac{a_i}{r} - a_e + 2 \left(a_e e^{-x_0^2} - \frac{a_i}{r} e^{-r^2 x_0^2} \right) \right],$$

with x_0 taken from (5.5). Figure 7 shows plots of thresholds v_{thr} with respect to the parameter r for two parameter couples of a_e, a_i . It turns out that condition (5.8) is fulfilled and oscillations are expected for a wide range of $r > 1$, whereas $r < 1$ (lateral inhibition) allows only for a small parameter regime. For appropriate parameters, the properties of the kernel and the temporal delays introduced by finite propagation speed interact in a way that destabilizes the stationary state and produces oscillations. Similar effects have also been found in previous works [6, 22].

Section 4 gives conditions for an oscillatory bifurcation in case of large propagation velocity. To obtain oscillating activity constant in space (case IIa), Figure 1(d) illustrates the conditions $r < 1$ and $-\hat{K}_1(0)/(\gamma v) > \max_k \hat{K}(k)$, implying

$$(5.9) \quad \frac{a_e - a_i/r}{\gamma v \sqrt{\pi}} > a_e e^{-k_0^2/4} - a_i e^{-k_0^2/4r^2},$$

where k_0 is taken from (5.7). Figure 8 displays the corresponding spatiotemporal activity for appropriate parameters. From the figure, an oscillation frequency of about $\omega = 0.28$ can be observed. This agrees well with the theory, as from (3.10)

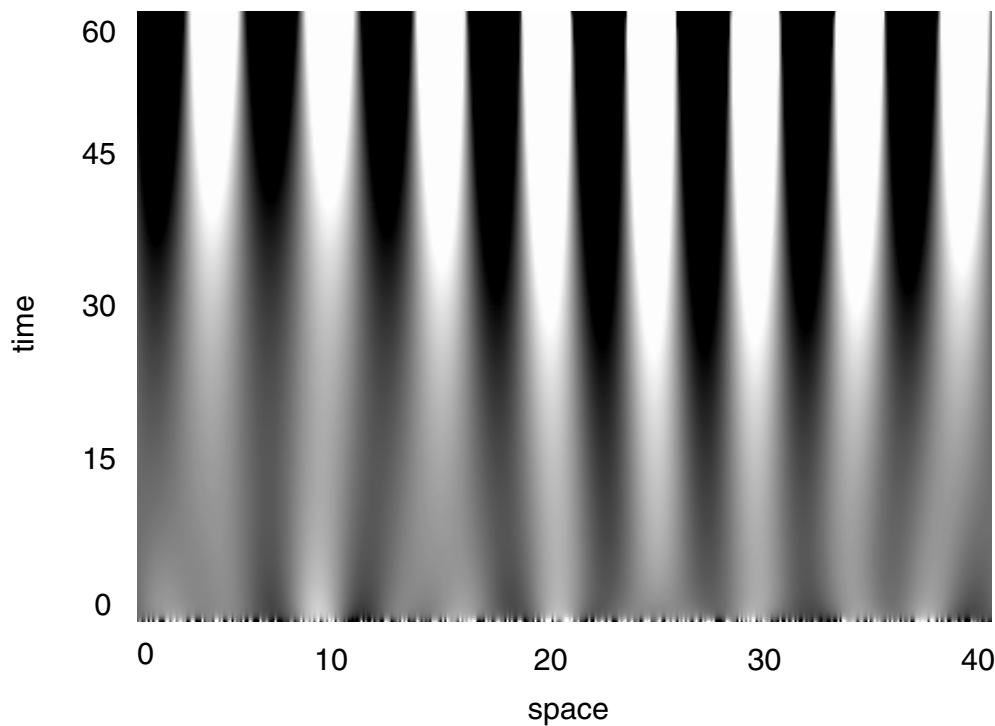


FIG. 6. Space-time plot of the Turing instability, obtained for the Gaussian connectivity kernel and parameters $E^* = 0.74$, $r = 0.5$, $\gamma = 2$, $a_e = 60$, $a_i = 55$, $v = 100$, $\beta = 1$, $N = 400$, and $1/\alpha = 0.727$. Initial conditions $V^0(x, t)$ are chosen randomly from a uniform distribution on $[V^* - 0.1, V^* + 0.1]$ for $t \in [-l/v, 0]$, where $l = 40$.

with $c \geq 1$ a frequency in the interval $[0, 0.26]$ is predicted at the bifurcation. The small discrepancy arises from choosing the simulation parameters somewhat beyond the bifurcation values in order to obtain reasonably high amplitude solutions for visualization.

On the other hand, for traveling waves (case IIb) $k \neq 0$ and Figure 1(c) gives the conditions $r > a_e/a_i$ and $\max_k -\hat{K}_1(k)/(\gamma v) > \hat{K}(0)$. A series expansion for \hat{K}_1 [20] yields a single implicit condition for parameters a_e, a_i, r and k . Figure 9 shows the corresponding space-time plot of the wave instability for appropriate parameters. Here $r > 1$, and the field activity is shifted from local to lateral spatial locations, facilitating traveling waves.

Finally we examine how the phase velocity of traveling waves depends on the propagation velocity v in the system. From (4.10) the phase velocity reads

$$(5.10) \quad v_{\text{ph}} = \frac{\omega}{k^*} = \frac{v}{k^*} \sqrt{\frac{\alpha \hat{K}(k^*) - 1}{\frac{1}{2} \alpha \hat{K}_2(k^*) - v^2}},$$

where k^* solves (4.8). In Figure 10, v_{ph} is plotted and exhibits a slightly nonlinear dependence on the propagation velocity for the applied parameters. We point to the small ratio of phase velocity to propagation velocity in accordance with previous findings [32, 23].

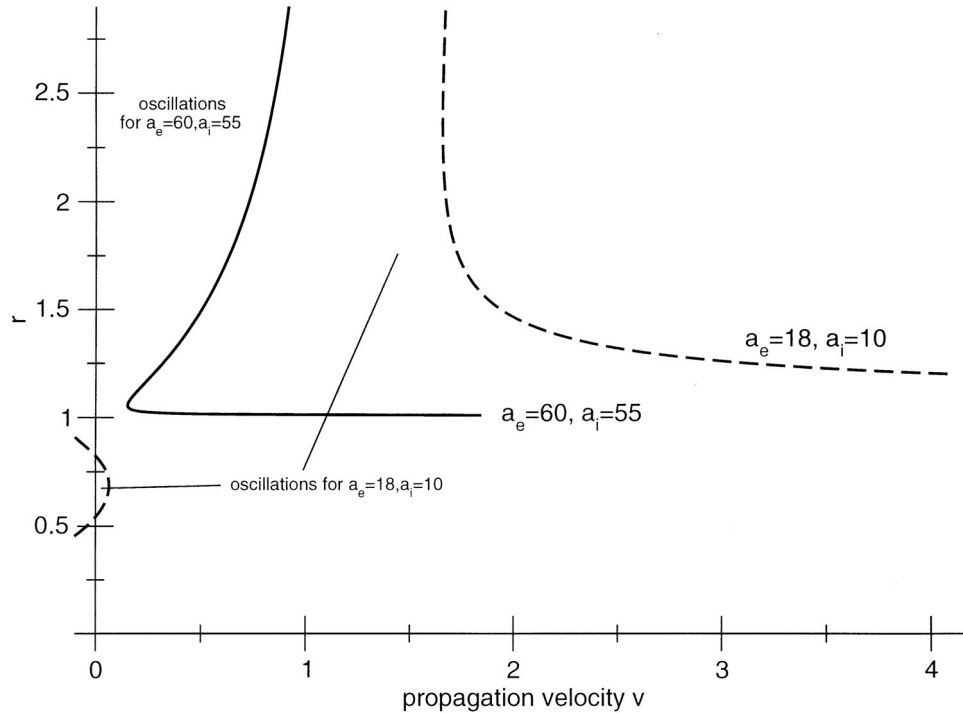


FIG. 7. Thresholds of oscillatory phenomena v_{thr} for two parameter sets a_e, a_i . The sufficient condition for oscillations is fulfilled for $v < v_{\text{thr}}$, i.e., the left-hand side of each curve.

6. Conclusion. We have presented an analysis of the stability of equilibrium solutions for a general class of neural field equations on the real line. The details of bifurcations arising from loss of stability provide important information concerning a variety of dynamical behavior that is of neuroscientific interest, including spatial patterns and traveling waves. The stationary bifurcations and the resulting spatial patterns depend only on the connectivity kernel, and are completely determined by its Fourier transform $\hat{K}(k)$. On the other hand, the axonal delays due to finite propagation speed are shown to have significant effects on the nonstationary bifurcations. In fact, we have proved that in first- and second-order systems, nonstationary bifurcations of equilibria can occur only if the delays are sufficiently large, that is, when the transmission speed is sufficiently small. This behavior is different from that of higher order systems, where nonstationary bifurcations can occur even in the absence of delays. By a perturbation approach we have expressed the conditions for bifurcation in terms of the Fourier transforms of the moments of the kernel function. For high signal transmission speeds, only the first kernel moment needs to be considered to draw qualitative conclusions. For first- and second-order systems this leads to a simple method for determining the possible bifurcation types by comparing the Fourier transforms $\hat{K}(k)$ and $-\hat{K}_1(k)/v\gamma$. Furthermore, the bifurcations depend only on the extremal values of the transforms, rather than the precise shapes of the kernels.

The analysis presented here, being applicable to a broad range of connectivity and synaptic properties and transfer functions, suggests some general conclusions on the types of nonlinear dynamics that can be observed in a fairly wide class of systems.

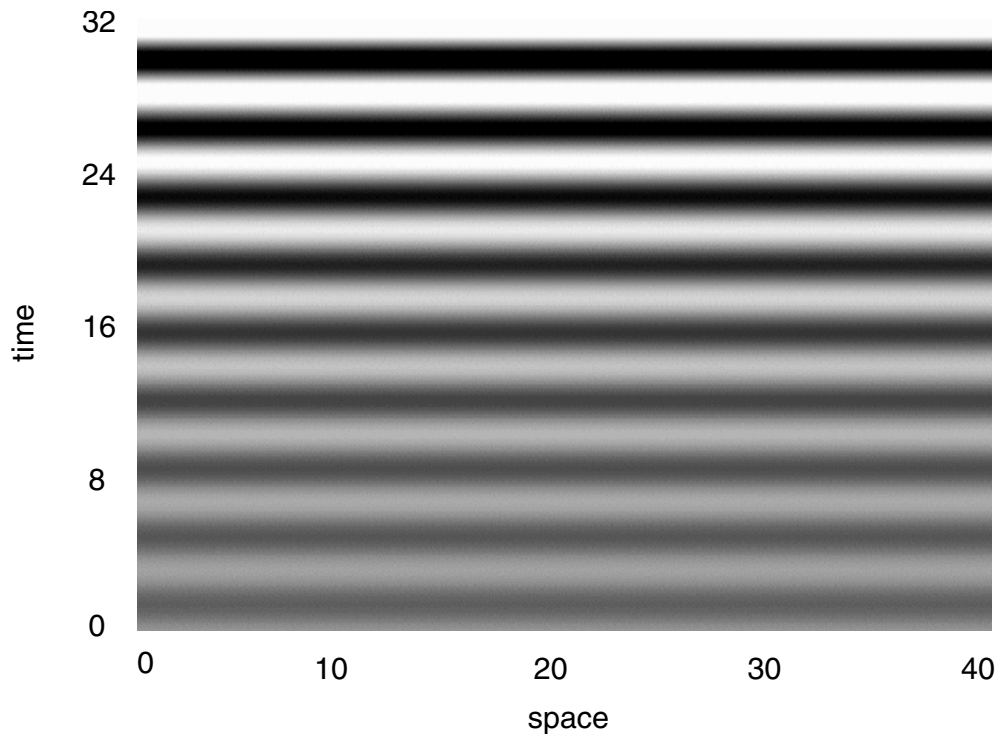


FIG. 8. Space-time plot of the Hopf instability leading to periodic oscillations of a spatially constant solution (type IIa bifurcation), obtained for the Gaussian connectivity kernel and parameters $E^* = 0.91$, $r = 0.2$, $\gamma = 0.5$, $a_e = 18$, $a_i = 10$, $v = 6$, $\beta = 1$, $N = 400$. Initial conditions are $V^0(x, t) = V^* + 0.02$ for $t \in [-l/v, 0]$, with $V^* = 0.11$ and $l = 40$.

For instance, one generally expects to see oscillatory behavior whenever the signal transmission speed is sufficiently small. In fact, for completely general kernels, the peaks of $\hat{K}(k)$ and $-\hat{K}_1(k)$ are more likely to occur at some nonzero k rather than at the precise value $k = 0$. This suggests that in first- and second-order systems the prevalent dynamics arising from bifurcations of equilibria will be either spatial patterns or traveling waves, depending on whether the transmission speed is large or small, respectively. Nevertheless, more specific kernel types may dictate different dynamical behavior depending on the application.

There are many studies of discrete networks which exhibit in-phase periodic behavior by increased constant delay (e.g., [49, 6]) and propagation delay (e.g., [17, 26, 22]). These studies consider specific network connectivities and obtain similar results with respect to the role of delays in oscillatory behavior. In this context, we would like to mention the recent work of Earl and Strogatz [9], who studied the stability of discrete, homogeneous oscillator networks with constant connection delays. They obtain a rather strong stability condition for global in-phase oscillations that is independent of the connectivity topology, provided each node has the same number of connections. The in-phase oscillations correspond to type IIa bifurcations in our study; however, we also have the possibility of other bifurcation types, indicating that the neural fields considered here can exhibit a richer range of dynamics. An important difference arises from the nature of the delays in the two models. In the discrete network with a constant connection delay, each unit knows the state of its neighbors

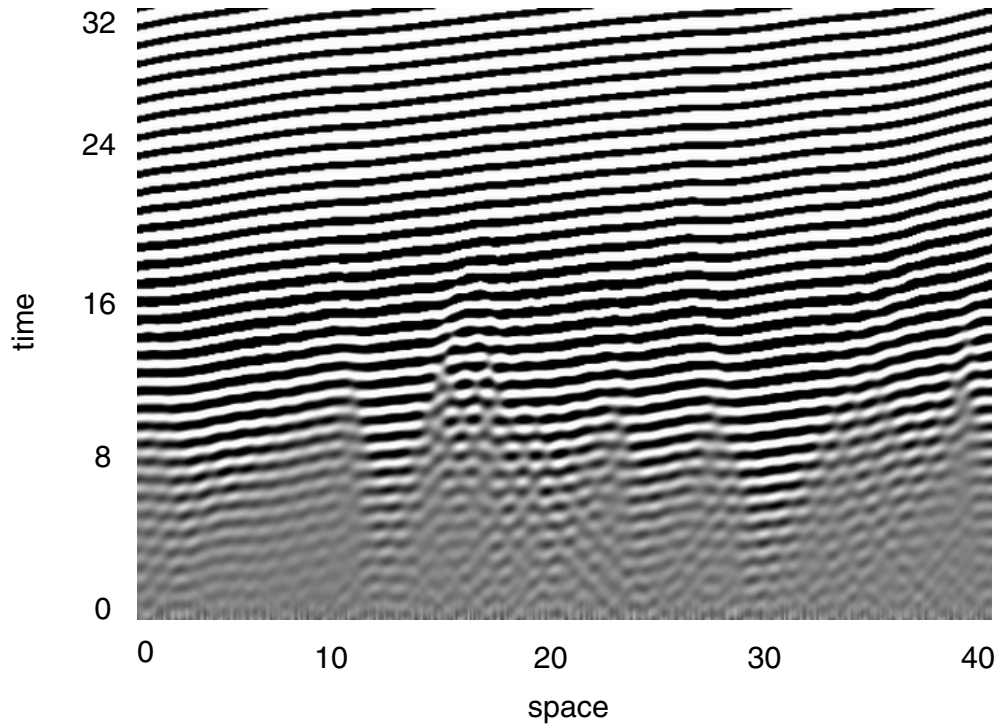


FIG. 9. Space-time plot of the wave instability (type IIb bifurcation), obtained for the Gaussian connectivity kernel and parameters $E^* = 1.29$, $r = 3$, $\gamma = 2$, $a_e = 60$, $a_i = 55$, $v = 1$, $\beta = 1$, $N = 400$. Initial conditions $V^0(x, t)$ are chosen randomly from a uniform distribution on $[V^* - 0.1, V^* + 0.1]$ for $t \in [-l/v, 0]$, where $l = 40$.

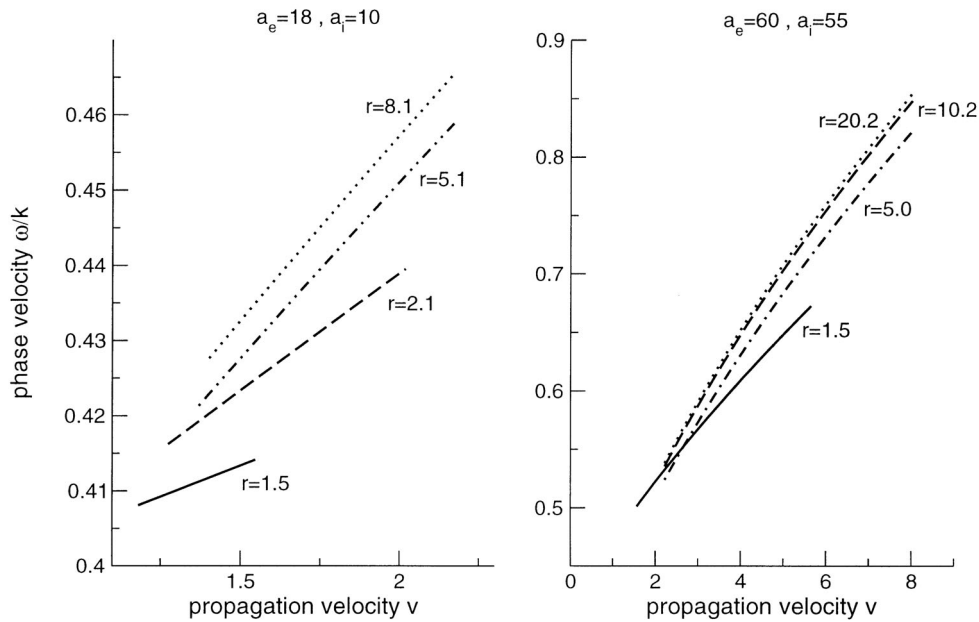


FIG. 10. The wave velocity of traveling waves with respect to axonal propagation velocity. Parameters are $\gamma = 0.2$, $0.03 \leq \alpha \leq 0.11$ and $\omega/v \approx 0.7$ (left, for $v \approx 2$) and $\omega/v \approx 0.3$ (right, for $v \approx 7$), respectively.

at the same time instant (although not at the present time), so it is plausible that this type of arrangement favors in-phase oscillations. On the other hand, our model involves distance-dependent delays, for which travelling waves may be the more natural type of oscillatory behavior. The details of this interesting connection will be given in a future paper.

Our work is mostly motivated by experimental findings (e.g., [29, 44, 16]). In this line, the presented study aims to generalize the analysis of synaptically coupled neuronal fields in order to gain a classification scheme for observed spatiotemporal patterns. Here, we would like to mention the important generalization of Amari [1] in lateral-inhibition-type fields without axonal delay. Since neurophysiological properties of observed neural tissue are not accessible precisely, a classification scheme might link model functionals with observed phenomena. For example, observed traveling waves necessitate an axonal propagation velocity below a certain threshold defined by connectivity kernel properties and synaptic response properties (Theorem 3.1), and furthermore, their frequencies are confined to a bounded band (Theorem 3.2). In addition, this classification might be important for estimating interaction parameters from multisite neuronal data (e.g., [14]). Due to the large number of different activity phenomena, further studies in this area could incorporate additional mechanisms like standing and traveling pulse fronts as in [32, 33], boundary effects in local neuronal areas (e.g., [7]), the influence of external inputs [45, 10] local in space and time, or the constant delayed feedback found experimentally in thalamocortical connections [41] and visual areas [27, 11] and which has been addressed in several theoretical studies (e.g., [13, 5, 3]). In particular, the mutual treatment of both constant delayed feedback and propagation delay proposes new insights into information processing between distant brain areas. Moreover, consideration of neural fields in higher space dimensions might yield further interesting results.

Acknowledgment. We thank Matthew P. James for a critical reading of the manuscript.

REFERENCES

- [1] S. AMARI, *Dynamics of pattern formation in lateral-inhibition type neural fields*, Biol. Cybernetics, 27 (1977), pp. 77–87.
- [2] G. G. BLASDEL AND G. SALAMA, *Voltage-sensitive dyes reveal a modular organization in monkey striate cortex*, Nature, 321 (1986), pp. 579–585.
- [3] P. C. BRESSLOFF, *Synaptically generated wave propagation in excitable neural media*, Phys. Rev. Lett., 82 (1999), pp. 2979–2982.
- [4] P. C. BRESSLOFF, *Traveling waves and pulses in a one-dimensional network of excitable integrate-and-fire neurons*, J. Math. Biol., 40 (2000), pp. 169–198.
- [5] P. C. BRESSLOFF AND S. COOMBES, *Physics of the extended neuron*, Internat. J. Modern Phys. B, 11 (1997), pp. 2343–2392.
- [6] N. BRUNEL AND V. HAKIM, *Fast global oscillations in networks of integrate-and-fire neurons with low firing rates*, Neural Comput., 11 (1999), pp. 1621–1671.
- [7] C. CAVADA AND P. S. GOLDMAN-RAKIC, *Multiple visual areas in the posterior parietal cortex of primates*, Prog. Brain Res., 95 (1993), pp. 123–137.
- [8] S. COOMBES, G. J. LORD, AND M. R. OWEN, *Waves and bumps in neuronal networks with axo-dendritic synaptic interactions*, Phys. D, 178 (2003), pp. 219–241.
- [9] M. G. EARL AND S. H. STROGATZ, *Synchronization in oscillator networks with delayed coupling: A stability criterion*, Phys. Rev. E, 67 (2003), p. 036204.
- [10] M. ENCULESCU AND M. BESTEHORN, *Activity dynamics in nonlocal interacting neural fields*, Phys. Rev. E, 67 (2003), p. 041904.
- [11] A. K. ENGEL, P. KOENIG, A. K. KREITER, AND W. SINGER, *Interhemispheric synchronization of oscillatory neuronal responses in cat visual cortex*, Science, 252 (1991), pp. 1177–1179.

- [12] B. ERMENTROUT, *Neural networks as spatio-temporal pattern-forming systems*, Rep. Progr. Phys., 61 (1998), pp. 353–430.
- [13] U. ERNST, K. PAWELZIK, AND T. GEISEL, *Delay-induced multi-stable synchronization of biological oscillators*, Phys. Rev. E, 57 (1998), pp. 2150–2162.
- [14] O. FRANÇOIS, C. LAROTA, J. HORIKAWA, AND T. HERVÉ, *Diffusion and innovation rates for multidimensional neuronal data with large spatial covariances*, Network: Comput. Neural Syst., 11 (2000), pp. 211–220.
- [15] W. J. FREEMAN, *Characteristics of the synchronization of brain activity imposed by finite conduction velocities of axons*, Int. J. Bif. Chaos, 10 (2000), pp. 2307–2322.
- [16] W. J. FREEMAN, *Neurodynamics: An Exploration in Mesoscopic Brain Dynamics*, Perspectives in Neural Computing, Springer-Verlag, Berlin, 2000.
- [17] W. GERSTNER, *Rapid phase locking in systems of pulse-coupled oscillators with delays*, Phys. Rev. Lett., 76 (1996), pp. 1755–1758.
- [18] P. S. GOLDMAN-RAKIC, *Cellular basis of working memory*, Neuron, 14 (1995), pp. 477–485.
- [19] D. GOLOMB AND G. B. ERMENTROUT, *Effects of delay on the type and velocity of travelling pulses in neuronal networks with spatially decaying connectivity*, Network: Comput. Neural Syst., 11 (2000), pp. 221–246.
- [20] I. S. GRADSHTEYN AND I. M. RYZHIK, *Table of Integrals, Series, and Products*, Academic Press, San Diego, 2000.
- [21] A. GRINDVALD, L. ANGLISTER, J. A. FREEMAN, R. HILDESHEIM, AND A. MANKER, *Real-time optical imaging of naturally evoked electrical activity in intact frog brain*, Nature, 308 (1984), pp. 848–850.
- [22] H. HAKEN, *Effect of delay on phase locking in a pulse coupled neural network*, Eur. Phys. J. B, 18 (2000), pp. 545–550.
- [23] A. HUTT, M. BESTEHORN, AND T. WENNEKERS, *Pattern formation in intracortical neuronal fields*, Network: Comput. Neural Syst., 14 (2003), pp. 351–368.
- [24] V. K. JIRSA AND H. HAKEN, *A derivation of a macroscopic field theory of the brain from the quasi-microscopic neural dynamics*, Phys. D, 99 (1997), pp. 503–526.
- [25] V. K. JIRSA, K. J. JANTZEN, A. FUCHS, AND J. A. S. KELSO, *Spatiotemporal forward solution of the EEG and MEG using network modelling*, IEEE Trans. Medical Imaging, 21 (2002), pp. 493–504.
- [26] W. M. KISTLER, R. SEITZ, AND J. L. VAN HEMMEN, *Modeling collective excitations in cortical tissue*, Phys. D, 114 (1998), pp. 273–295.
- [27] L. A. KRUBITZER AND J. H. KAAS, *Cortical integration of parallel pathways in the visual system of primates*, Brain Res., 478 (1987), pp. 161–165.
- [28] J. W. LANCE, *Current concepts of migraine pathogenesis*, Neurology, 43 (1993), pp. S11–S15.
- [29] P. L. NUNEZ, *Neocortical dynamics and human EEG rhythms*, Oxford University Press, New York, Oxford, 1995.
- [30] P. L. NUNEZ, *Toward a quantitative description of large-scale neocortical dynamic function and EEG*, Behav. Brain Sci., 23 (2000), pp. 371–437.
- [31] R. OSAN AND G. B. ERMENTROUT, *The evolution of synaptically generated waves in one- and two-dimensional domains*, Phys. D, 163 (2002), pp. 217–235.
- [32] D. J. PINTO AND G. B. ERMENTROUT, *Spatially structured activity in synaptically coupled neuronal networks: I. Travelling fronts and pulses*, SIAM J. Appl. Math., 62 (2001), pp. 206–225.
- [33] D. J. PINTO AND G. B. ERMENTROUT, *Spatially structured activity in synaptically coupled neuronal networks: II. Lateral inhibition and standing pulses*, SIAM J. Appl. Math., 62 (2001), pp. 226–243.
- [34] C. J. RENNIE, P. A. ROBINSON, AND J. J. WRIGHT, *Unified neurophysical model of EEG spectra and evoked potentials*, Biol. Cybernetics, 86 (2002), pp. 457–471.
- [35] P. A. ROBINSON, P. N. LOXLEY, S. C. O’CONNOR, AND C. J. RENNIE, *Modal analysis of corticothalamic dynamics, electroencephalographic spectra and evoked potentials*, Phys. Rev. E, 63 (2001), p. 041909.
- [36] P. A. ROBINSON, C. J. RENNIE, AND J. J. WRIGHT, *Propagation and stability of waves of electrical activity in the cerebral cortex*, Phys. Rev. E, 56 (1997), pp. 826–840.
- [37] B. M. SALZBERG, H. V. DAVILA, AND L. B. COHEN, *Optical recording of impulses in individual neurons of an invertebrate central nervous system*, Nature, 246 (1973), pp. 508–509.
- [38] H. G. SCHUSTER AND P. WAGNER, *A model for neuronal oscillations in the visual cortex: 1. Mean-field theory and derivation of the phase equations*, Biol. Cybern., 64 (1990), pp. 77–82.
- [39] W. SINGER AND C. M. GRAY, *Visual feature integration and the temporal correlation hypothesis*, Ann. Rev. Neurosci., 18 (1995), pp. 555–586.

- [40] H. SPORS AND A. GRINDVALD, *Spatio-temporal dynamics of odor representations in the mammalian olfactory bulb*, *Neuron*, 34 (2002), pp. 301–315.
- [41] M. STERIADE, E. G. JONES, AND R. R. LLINAS, *Thalamic Oscillations and Signalling*, Wiley, New York, 1990.
- [42] A. K. STURM AND P. KÖNIG, *Mechanisms to synchronize neuronal activity*, *Biol. Cybernet.*, 84 (2001), pp. 153–172.
- [43] P. TASS, *Oscillatory cortical activity during visual hallucinations*, *J. Biol. Phys.*, 23 (1997), pp. 21–66.
- [44] C. UHL, ED., *Analysis of Neurophysiological Brain Functioning*, Springer-Verlag, Berlin, 1999.
- [45] T. WENNEKERS, *Dynamic approximation of spatio-temporal receptive fields in nonlinear neural field models*, *Neural Comput.*, 14 (2002), pp. 1801–1825.
- [46] H. R. WILSON AND J. D. COWAN, *A mathematical theory of the functional dynamics of cortical and thalamic nervous tissue*, *Kybernetik*, 13 (1973), pp. 55–80.
- [47] J. J. WRIGHT AND R. R. KYDD, *The electroencephalogram and cortical neural networks*, *Network*, 3 (1992), pp. 341–362.
- [48] J. Y. WU, L. GUAN, AND Y. TSAU, *Propagating activation during oscillations and evoked responses in neocortical slices*, *J. Neurosci.*, 19 (1999), pp. 5005–5015.
- [49] M. K. S. YEUNG AND S. H. STROGATZ, *Time delay in the Kuramoto model of coupled oscillators*, *Phys. Rev. Lett.*, 82 (1999), pp. 648–651.